

Excitonic wave-packet evolution in a two-orbital Hubbard model chain: A real-time real-space study

Bradraj Pandey^{1,2}, Gonzalo Alvarez³, and Elbio Dagotto^{1,2}

¹*Department of Physics and Astronomy, University of Tennessee, Knoxville, Tennessee 37996, USA*

²*Materials Science and Technology Division, Oak Ridge National Laboratory, Oak Ridge, Tennessee 37831, USA*

³*Computational Sciences & Engineering Division and Center for Nanophase Materials Sciences,
Oak Ridge National Laboratory, Oak Ridge, Tennessee 37831, USA*

Motivated by experimental developments introducing the concept of spin-orbit separation, we study the real-space time evolution of an excitonic wave-packet using a two-orbital Hubbard model. The exciton is created by exciting an electron from a lower energy half-filled orbital to a higher energy empty orbital. We carry out the real-time dynamics of the resulting excitonic wave-packet, using the time-dependent density matrix renormalization group method. We find clear evidence of charge-spin and spin-orbit separation in real-space, by tracking the time evolution of local observables. We show that the velocity of the orbiton can be tuned by varying the inter-orbital interactions. We also present a comparative study of a hole (in one orbital) and exciton (in two orbitals) dynamics in one-dimensional systems. Moreover, we analyze the dynamics of an exciton with spin-flip excitation, where we observe fractionalized spinons induced by Hund's interaction.

Introduction. The dynamics of excitations in low-dimensional compounds has attracted considerable attention [1, 2]. Experimentally observed excitations include holons, spinons, doublons, and excitons [3, 4]. In particular, the study of excitons in multiband insulators unveiled interesting surprises [5, 6]. Localized and delocalized charge-transfer excitons were observed experimentally in La_2CuO_4 and La_2NiO_4 , respectively [7]. More recently, spin-orbit excitons were observed in Sr_2IrO_4 using Resonant Inelastic X-ray Scattering (RIXS) [8]. The excitonic dynamic in Sr_2IrO_4 was described as analogous to the propagation of holes in a cuprate's antiferromagnetic (AFM) background [9].

Due to reduced dimensionality and strong correlation effects, quasi one-dimensional (1D) systems display exotic dynamical properties [10–12], including the fractionalization of low-energy excitations [1, 3] into spin (spinons) and charge (holons) excitations propagating with different velocities [13–15]. The existence of spin-charge separation was shown experimentally early on in quasi one-dimensional systems [16, 17]. Interestingly, the fractionalization of electronic excitations is not limited only to spin and charge, but it can also include the orbital degree of freedom. In fact, spin-orbital separation was observed experimentally in the transition metal compound Sr_2CuO_3 [18]. Using high-resolution RIXS experiments, spin-orbital separation was also observed in the ladder system CaCu_2O_3 [19].

Recently, the spin-orbit separation in Mott insulating systems was studied theoretically using the effective Kugel-Khomskii model [20]. In the limit of vanishing Hund's coupling, the propagation of the orbiton in a ferro-orbital and antiferro-magnetic chain was shown to map into a "single hole" moving in an AFM chain with its dynamics described by an effective $t - J$ model [20]. However, in transition metal compounds, the Hund interaction plays an important role and, depending on the ma-

terial, it can be strong. Precisely for a strong Hund's coupling, the propagation of an orbiton, with inter-orbital FM and AFM spin alignments (in the excited states of the superexchange process) are not equal, and the simple mapping between orbiton and $t - J$ hole dynamics is no longer valid [21, 22]. More recently, using RIXS the impact of the Hund's interaction on the orbiton propagation of the quasi-1D AFM compound Ca_2CuO_2 was studied [22]. It was observed that robust Hund's interactions are required in the theoretical description to understand the experimental orbital spectrum [22].

In this letter, we provide the first study of spin-orbit separation in a real-time and real-space formalism by creating a finite momentum excitonic wave-packet at time $t = 0$, using a one-dimensional chain with two orbitals at each site. This wave-packet is created by exciting an electron from a half-filled orbital to an empty higher-energy orbital, as in experiments. Previous studies primarily focused on the spectral properties to study spin-orbit separation and for simplicity relied on Kugel-Khomskii models in the strong coupling limit [20, 21]. Here we consider a more general multi-orbital Hubbard Hamiltonian at intermediate coupling strengths, accounting also for charge fluctuations and with focus on the influence of the Hund's coupling. To study the excitonic real-time dynamics, we use the time-dependent density-matrix-renormalization group (t-DMRG) method [23, 24]. We have observed that after creating the exciton, the hole (in the half-filled orbital) and the electron (in the empty orbital) always move together, while the spin wave-packet in the half-filled orbital independently evolves from the charge wave-packet. We also compare the dynamics of a hole in a one-orbital chain versus the dynamics of an exciton in a two-orbital chain. Overall, at intermediate coupling and for robust values of the Hund's interaction, we find clear evidence of spin-orbit separation as time grows. Moreover, we quantitatively study the relation between the

Hund's coupling and the orbitalon velocity, finding that this orbitalon's velocity increases with an increase in the Hund's coupling magnitude, while the spinon's velocity remains unaffected. Furthermore, we also present the dynamics of a spin-flip exciton (the previous discussion was for a spin preserving exciton), where we find fractionalized spinons, induced by the strong Hund's coupling.

Model and Method. We use the two-orbital Hubbard model on a chain. The model can be written as the sum of kinetic and interaction energy terms $H = H_k + H_{in}$ [25]. The kinetic (tight-binding) portion contains the nearest-neighbor hopping along the chain direction defined as:

$$H_k = -t_{hop} \sum_{\langle ij \rangle, \sigma, \gamma} \left(c_{i\sigma\gamma}^\dagger c_{j\sigma\gamma} + H.c. \right) + \sum_{i, \gamma, \sigma} \Delta_\gamma n_{i\sigma\gamma} \quad (1)$$

where $c_{i\sigma\gamma}^\dagger$ creates an electron at the chain site i , with spin z -axis projection σ , and on orbital γ (either orbital a or b). t_{hop} is the hopping integral. For simplicity, we considered only intra-orbital hoppings along the chain and we used identical hopping for both orbitals [$t_a = t_b = t_{hop} = 1$]. Δ_γ denotes the crystal field term and $n_{i\sigma\gamma}$ is the orbital-resolved number operator at site i . We fix the crystal-field parameters as $\Delta_a = 4.1$ and $\Delta_b = 0$. The large crystal field $\Delta_a = 4.1 \gtrsim 4t_{hop}$ ensures only orbital b is occupied in the non-interacting ground state because the bandwidth W of orbital a is $W = 4t_{hop}$.

The electronic interaction portion is canonical:

$$H_{in} = U \sum_{i, \gamma} n_{i\uparrow\gamma} n_{i\downarrow\gamma} + \left(U' - \frac{J_H}{2} \right) \sum_{i, \gamma < \gamma'} n_{i\gamma} n_{i\gamma'} - 2J_H \sum_{i, \gamma < \gamma'} \mathbf{S}_{i\gamma} \cdot \mathbf{S}_{i\gamma'} + J_H \sum_{i, \gamma < \gamma'} \left(P_{i\gamma}^\dagger P_{i\gamma'} + H.c. \right). \quad (2)$$

The first term is the on-site Hubbard repulsion between \uparrow and \downarrow electrons in the same orbital. The second term is the electronic repulsion between electrons at different orbitals. The standard relation $U' = U - 2J_H$ is here assumed. The third term is the ferromagnetic Hund's interaction between electrons occupying the active two orbitals $\gamma = a, b$ of the same site. $\mathbf{S}_{i\gamma}$ is the total spin of orbital γ at site i . The last term is the pair-hopping between different orbitals, where $P_{i\gamma} = c_{i\downarrow\gamma} c_{i\uparrow\gamma}$.

To obtain the ground state $|\Psi_0\rangle$ of this model, we employed the static DMRG method. For our numerical calculations, we use a system size $L = 36$ with two orbitals at each site and we kept $m = 1200$ states. The exciton Gaussian wave-packet is created with spin σ and a crystal momentum k_0 , by applying the operator

$$h_\sigma^\dagger(k_0) = A \sum_j e^{-(j-j_0)^2/2\omega_r^2} e^{-ik_0 j} c_{j\sigma a}^\dagger c_{j\sigma b} \quad (3)$$

to the ground state $|\Psi_0\rangle$. This operator excites an electron from the half-filled orbital b to the empty orbital a , centered at site $i_0 = 18$ and with width $\omega_r = 2.54$. The

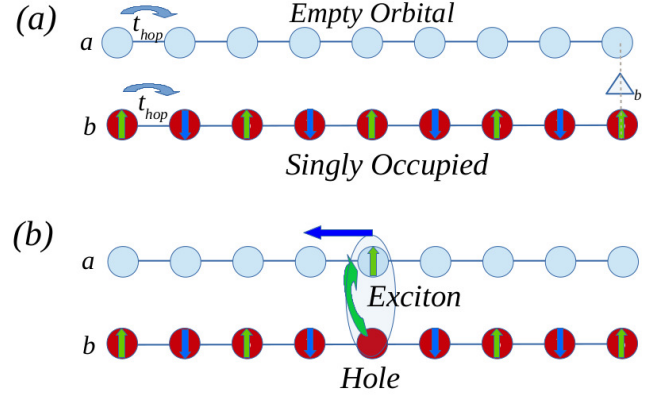


FIG. 1. Schematic representation of a one-dimensional chain with two orbitals (a and b) at each site. The blue circle represents orbital a and the red circle orbital b . (a) The orbitals are separated by a large crystal field Δ . Orbital b is half-filled, whereas orbital a is empty. (b) At $t = 0$ an exciton is created by exciting an electron from the half-filled orbital b (i. e., one electron per site in a staggered spin pattern) to orbital a which is empty. The exciton has a finite momentum k_0 indicated by the blue arrow.

number 2.54 implies the size of the initial Gaussian is exactly six lattice spacings at half height, a size that we considered adequate for easy visualization. A is the normalization constant of the Gaussian wave-packet. Due to the finite width $\omega_k = 1/2\pi\omega_r$ of the Gaussian wave-packet in momentum space, we fix the crystal momentum at $k_0 = -0.5\pi + 4\omega_k$ (i. e., close to the highest occupied electronic level with width $\omega_k = 0.06$). Because we construct a wave packet with a net nonzero momentum [$\mathbf{k}_0(\text{exciton}) = \mathbf{k}_e(\text{electron}) + \mathbf{k}_h(\text{hole})$ at time $t = 0$] that points in our case towards the left, the resulting time evolution will *not* be left-right symmetric.

We investigate numerically the time evolution of the one-exciton state $|\Psi_e\rangle = h_\sigma^\dagger(k_0)|\Psi_0\rangle$ under the influence of H i.e. $|\Psi(t)\rangle = e^{-iHt}|\Psi_e\rangle$. To perform the time evolution, we have implemented the Krylov space decomposition in the DMRG code [26, 27]. For the DMRG calculations, at least 1200 states were kept during the time evolution.

To study the dynamics of the excitonic wave-packet, we measure the following observables at each time step:

$$\langle n_{ia}(t) \rangle = \langle \Psi(t) | n_{ia\uparrow} + n_{ia\downarrow} | \Psi(t) \rangle \quad (4)$$

$$\langle n_{ib}(t) \rangle = \langle \Psi(t) | n_{ib\uparrow} + n_{ib\downarrow} | \Psi(t) \rangle \quad (5)$$

$$\langle S_{ia}^z(t) \rangle = \langle \Psi(t) | (n_{ia\uparrow} - n_{ia\downarrow}) / 2 | \Psi(t) \rangle \quad (6)$$

$$\langle S_{ib}^z(t) \rangle = \langle \Psi(t) | (n_{ib\uparrow} - n_{ib\downarrow}) / 2 | \Psi(t) \rangle \quad (7)$$

$$\langle \tau_{zi}(t) \rangle = \langle \Psi(t) | n_{ia} - n_{ib} | \Psi(t) \rangle \quad (8)$$

where $\langle n_{ia}(t) \rangle$ and $\langle n_{ib}(t) \rangle$ are the orbital-resolved time dependent charge densities of orbitals a and b . $\langle S_{ia}^z(t) \rangle$ and $\langle S_{ib}^z(t) \rangle$ are the respective orbital-resolved z -component of the time dependent spin densities. $\langle \tau_{zi}(t) \rangle$

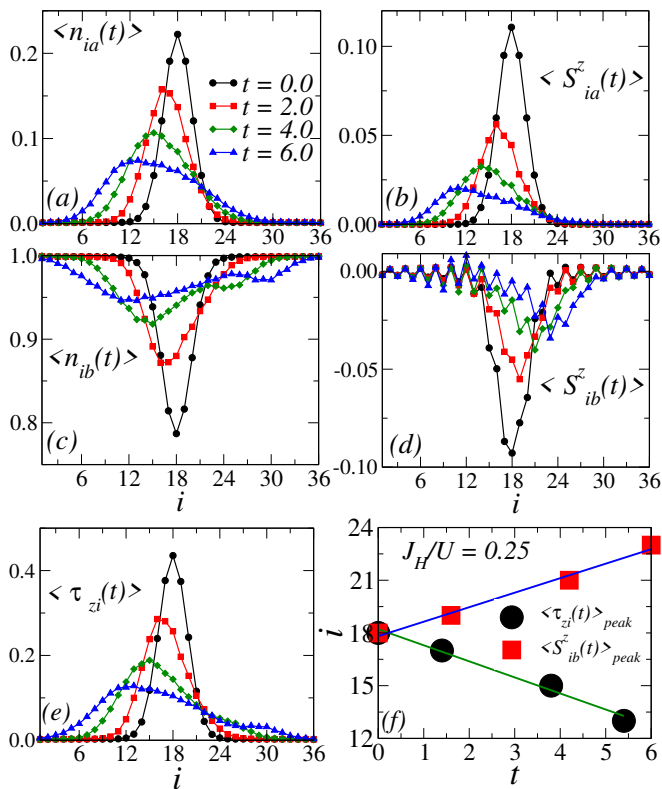


FIG. 2. Snapshots of the evolution of wave-packets at different times: (a) charge density $\langle n_{ib}(t) \rangle$, (b) charge density $\langle n_{ia}(t) \rangle$, (c) spin density $\langle S_{ib}^z(t) \rangle$, (d) spin density $\langle S_{ia}^z(t) \rangle$, and (e) orbital density $\langle \tau_{zi}(t) \rangle$. At $t = 0$, wave-packets are at the center of the system i.e. site $i_0 = 18$. (e) Positions of the peaks of the orbital (black circles) and spin (red squares) wave-packets vs. t . The peak positions are fitted with straight lines to extract the velocity of orbital and spin wave-packets. These results were obtained at $J_H/U = 0.25$ and $U/W = 1.0$ using t-DMRG for a $L = 36$ sites system.

is the z -component of the time-dependent orbital density. All these quantities are site dependent.

Results. The Hamiltonian ground state, at overall quarter-filling ($L = 36$ and total number of electrons $N_e = 36$) and parameters $U/W = 1.0$, $J_H/U = 0.25$ [28], and $\Delta_a = 4.1$, results in a situation where orbital b is a half-filled Mott-insulator with AFM-spin correlations, while orbital a remains empty. At time $t = 0$, the process previously described leads to an exciton centered in the middle of the chain, i.e. at site $i_0 = 18$. This results in a hole wave-packet $\langle n_{ib}(t) \rangle$ in orbital b [Fig. 2(a)] and an electron wave-packet $\langle n_{ia}(t) \rangle$ in orbital a [Fig. 2(c)]. The excitation of an electron from orbital b at $t = 0$ also creates spin-excitations $\langle S_{ia}^z(t) \rangle$ with up spins in orbital a [Fig. 2(b)] and down spins in orbital b $\langle S_{ib}^z(t) \rangle$ [Fig. 2(d)].

As shown in Figs. 2(a) and (b), with increasing time the charge wave-packet $\langle n_{ia}(t) \rangle$ and the spin wave-packet $\langle S_{ia}^z(t) \rangle$ at orbital a (the originally empty orbital) move with similar speeds toward the left from the central site $i_0 = 18$, indicating no spin-charge separation for or-

bitals a , as expected for an electron moving in an empty medium. Interestingly, the charge wave-packets $\langle n_{ia}(t) \rangle$ and $\langle n_{ib}(t) \rangle$ move together, as mirror images of each other [see Figs. 2(a) and (c)]. The reason is that the inter-orbital interaction $U' = U - 2J_H$ acts as an effective attraction between the hole in orbital b and an electron in orbital a [29]. Intuitively, when the hole of orbital b and the electron in orbital a are in the same site, the strong inter-orbital repulsion energy U' is not active (as compared to the case where two electrons are on the same site). This results in the formation of an electron-hole bound pair exciton which moves together with increasing time t towards the left of site $i_0 = 18$. The charge wave-packet $\langle n_{ib}(t) \rangle$ and spin wave-packet $\langle S_{ib}^z(t) \rangle$ move in opposite directions with time, providing clear evidence of spin-charge separation [see Fig. 2(c) and (d)], in the half-filled orbital b .

In the electron-hole pair exciton, the electron promoted from the half-filled orbital b to the unoccupied orbital a is also equivalent to creating an *orbiton* [21, 30]. In Fig. 2(e), we show the orbiton dynamics via $\langle \tau_{zi}(t) \rangle$ evolving with time t . The orbital wave-packet $\langle \tau_{zi}(t) \rangle$ moves similarly to $\langle n_{ib}(t) \rangle$ and $\langle n_{ia}(t) \rangle$, towards the left from the central site $i_0 = 18$, while the spin wave-packet $\langle S_{ib}^z(t) \rangle$ moves toward the right. Thus, our result can be reinterpreted as a signature of spin-orbit separation in real-space with increasing time t . To determine the velocities of the orbital and spin excitations, we monitored the positions of the peak values of $\langle \tau_{zi}(t) \rangle$ and $\langle S_{ib}^z(t) \rangle$ vs. time. Using simple linear fits to extract the orbiton (v_τ) and spinon (v_s) velocities [Fig. 2(f)], we find that the orbital wave-packet ($v_\tau = -0.91$) has a speed only slight faster than the spin wave-packet ($v_s = 0.82$), at $J_H/U = 0.25$ and $U/W = 1.0$.

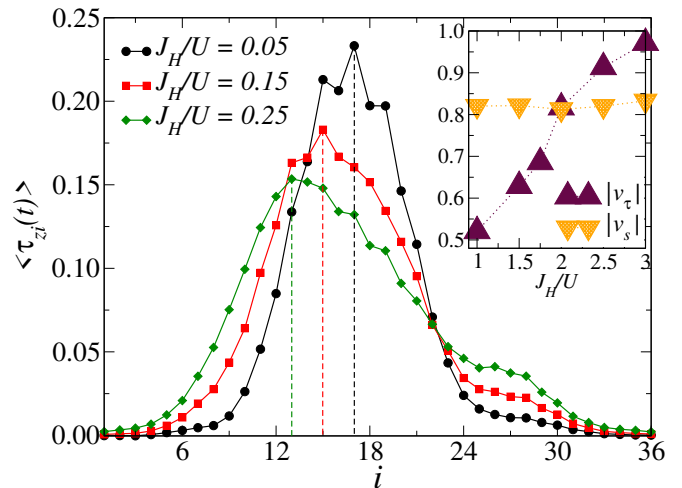


FIG. 3. Orbital density $\langle \tau_{zi}(t) \rangle$ at time $t = 5$ for three values of Hund's interactions J_H/U and at fixed $U/W = 1.0$. Inset: orbiton and spinon speeds $|v_\tau|$ and $|v_s|$ parametric with Hund's interaction J_H/U at $U/W = 1.0$.

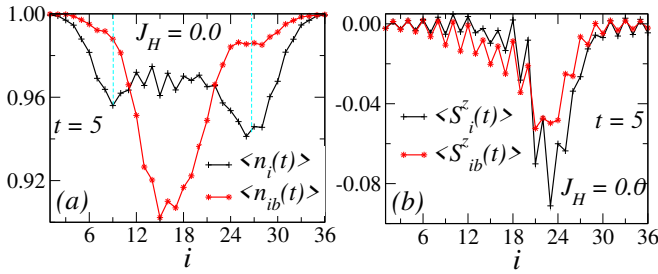


FIG. 4. Comparison of dynamics of a hole in the one-orbital (half-filled) and two-orbital (quarter-filled) 1D chain at $t = 5$. (a) Charge densities $\langle n_i(t) \rangle$ (one-orbital) and $\langle n_{ib}(t) \rangle$ (two-orbital) (b) Spin densities $\langle S_i^z(t) \rangle$ (one-orbital) and $\langle S_{ib}^z(t) \rangle$ (two-orbital).

Next, to study the role of the inter-orbital repulsion U' and Hund's coupling J_H in the dynamics of the exciton wave-packet, we calculate $\langle \tau_{zi}(t) \rangle$ and $\langle S_{ib}^z(t) \rangle$ for different values of J_H/U . Figure 3(a) displays the orbital wave-packet at time $t = 5$ but for three different values of J_H/U . We find that for the smaller coupling $J_H/U = 0.05$ the wave-packet $\langle \tau_{zi}(t) \rangle$ traveled only a very short distance from the central site $i_0 = 18$. However, increasing the Hund coupling to $J_H/U = 0.25$, still at time $t = 5$, $\langle \tau_{zi}(t) \rangle$ traveled a larger distance (five lattice spacings) from the central site $i_0 = 18$. The inset shows the orbital and spinon speeds $|v_\tau|$ and $|v_s|$, respectively, vs. J_H/U . We find that the orbital velocity increases significantly with increasing J_H/U . We believe this is because increasing J_H/U reduces the inter-orbital interaction U' , which results in a less-tightly bound electron-hole pair and, thus, the exciton becomes less heavier and can move at a faster rate $|v_\tau|$. On the other hand, at small J_H/U the inter-orbital interaction U' increases and results in heavier excitons, which naturally are more localized [7, 29]. The larger value of orbital velocity was observed in RIXS experiments because of the large Hund's coupling in Ca_2CuO_3 [22]. The increase in orbital velocity was explained in terms of the superexchange process [21, 22], where they showed that the energy of the intermediate state during the movement of the orbital depends on Hund's coupling J_H . For completeness, note that we find the spin speed $|v_s|$ (inset) does not change much with increasing J_H/U , and remains unaffected by the concomitant modifications in U' , which is intuitively reasonable.

In Figs. 4(a) and (b), we show a comparison of the dynamics of a hole in the one-orbital Hubbard model (half-filled chain, $U/W = 1.0$) and in the two-orbital Hubbard model (quarter-filled, $U/W = 1.0$, $U'/W = 1.0$, and $J_H/U = 0$) chain system. At $t = 0$, a hole was created at the central site $i_0 = 18$, either by removing an electron at site $i_0 = 18$ for the one-orbital case or, for two orbitals, removing an electron in orbital b and exciting this electron to orbital a at the same site

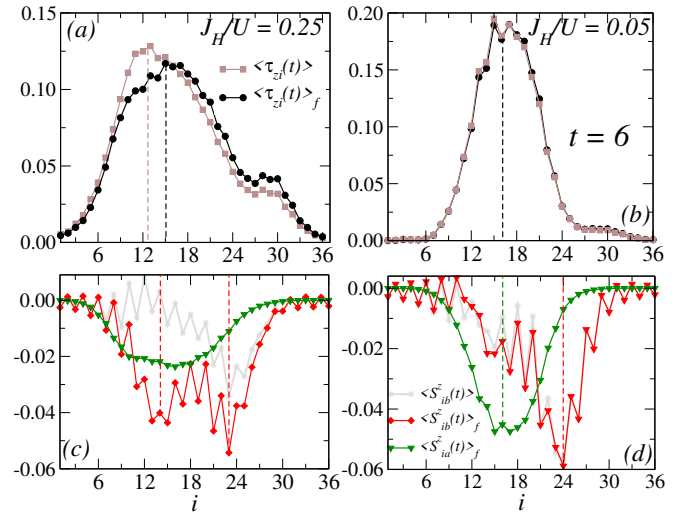


FIG. 5. Comparison of dynamics of exciton with and without spin-flip process. The orbital wave-packet with spin-flip (without spin flip) $\langle \tau_{zi}(t) \rangle_f$ ($\langle \tau_{zi}(t) \rangle$) is denoted by circles (squares). (a) is for $J_H/U = 0.25$ and (b) for $J_H/U = 0.05$. Spin wave-packets $\langle S_{ib}^z(t) \rangle_f$ (diamonds), $\langle S_{ia}^z(t) \rangle_f$ (down-triangle) with spin-flip process and $\langle S_{ib}^z(t) \rangle$ (stars) without spin-flip for (c) $J_H/U = 0.25$ and (d) $J_H/U = 0.05$. These results were obtained at time $t = 6$ and for $U/W = 1.0$.

$i_0 = 18$. The results for the charge wave-packets are remarkably different. While the charge wave-packet in the one-orbital system moves quite fast and splits into left and right moving wave-packets, the charge wave-packet in the two-orbital system moves very slowly due to the formation of the strong electron (in orbital a)-hole (in orbital b) bound state. The heaviness of the bound state electron-hole is natural because to propagate to the next site, it involves two hoppings t_a and t_b and an intermediate state with energy proportional to U [scale as $t_a t_b / U$], while the bare hole in one orbital propagates easily with just a hopping t_{hop} . Interestingly, the spin wave-packets in both systems move with a similar speed and towards the right from the central site $i_0 = 18$ [see Fig. 4(b)]. This is expected because after the separation of spin and charge wave packets in the two-orbital system (at quarter-filling), the spin moves approximately guided by the scale t_{hop}^2 / U , the same as the spinon follows in the one-orbital half-filled system [14].

In the RIXS experiment during the creation of orbital excitations spin-flip processes are also allowed [21, 22]. Figure 5 presents a comparison of orbital dynamics with and without spin-flip during the exciton generation, for different values of J_H/U . At $t = 0$, for the spin-flip process the exciton wave-packet was created by the operator $A \sum_j e^{-(j-j_0)^2 / 2\omega_r^2} e^{-ik_0 j} c_{j\downarrow a}^\dagger c_{j\uparrow b}$ acting on the ground state wave-function $|\Psi_0\rangle$. We found that the orbital velocity of $\langle \tau_{zi}(t) \rangle_f$ when spin flip occurs is only slightly reduced compared to the previously described spin non-flip case $\langle \tau_{zi}(t) \rangle$ at $J_H/U = 0.25$ [see Fig. 5(a)]. The

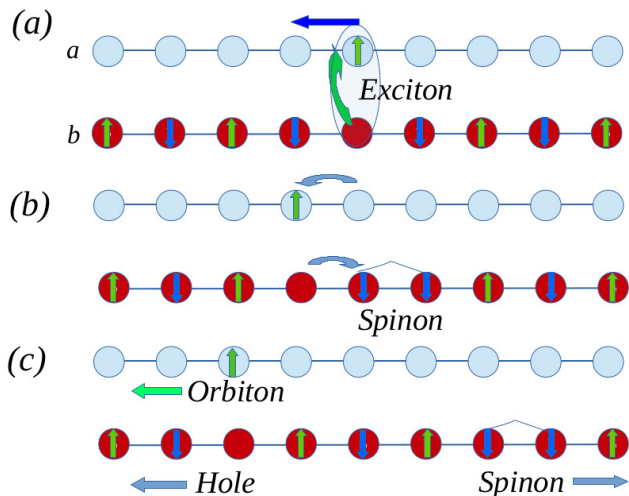


FIG. 6. Illustration of spin-orbit and spin-charge separation in a two-orbital (a and b) one-dimensional chain. (a) An exciton with a finite momentum (blue arrow) is created at $t = 0$ by exciting an electron from orbital b . (b) Electron in orbital a hops towards the left, while an electron with down spin on orbital b hops towards the right (i.e. hole moves to the left), creating a spinon on orbital b . (c) Orbital and hole move in a bound state to the left, while spinon moves free to the right.

slower speed of the spin-flip orbiton, compared to the spin-non-flip orbiton, is not expected from the superexchange picture [22] (where the spin-flip orbiton moves regulated by $t_a t_b / (U - 3J_H)$ and for spin non-flip case by $t_a t_b / (U - 2J_H)$) [31]. For a smaller $J_H/U = 0.05$, the results are almost identical and the orbital wave-packet moves very slowly in both cases [see Fig. 5(b)].

The spin-flip excitonic process leads to the creation of spin wave-packets $\langle S_{ib}^z(t) \rangle_f$ and $\langle S_{ia}^z(t) \rangle_f$ in the spin-down state [Fig. 5(c)]. Interestingly, at large J_H/U the spin-wave packet splits into two wave-packets with time ($t \gtrsim 3$), travelling in opposite directions (starting at the central site $i_0 = 18$). This curious splitting of the spin wave-packet $\langle S_{ib}^z(t) \rangle_f$ indicates the presence of two fractionalized spinons [32]. The left moving wave-packet $\langle S_{ib}^z(t) \rangle_f$ travels with similar speed as $\langle S_{ia}^z(t) \rangle_f$ of orbital a and $\langle \tau_{zi}(t) \rangle_f$. This could be due to the strong Hund's interaction between spin wave-packets of orbital a and b , which favors parallel alignment (spin-down state) of spin wave-packets $\langle S_{ib}^z(t) \rangle_f$ and $\langle S_{ia}^z(t) \rangle_f$. At large J_H/U , the creation of additional spinons was suggested in the spin-orbital spectrum [21]. In the case of spin-flip excitation, a strong J_H/U also leads to attraction between orbiton and spinon [21], which may be related to the slight slowdown of the orbiton velocity [Fig. 5(a)] compared to the without-spin-flip case (where spinon and orbiton repel each other [21]). The right moving spin-wave packet $\langle S_{ib}^z(t) \rangle_f$ moves with speed similar to that of $\langle S_{ib}^z(t) \rangle$ (without spin-flip case) [Fig. 5(c)]. On the other hand, for smaller J_H/U , the spin wave-packet $\langle S_{ib}^z(t) \rangle_f$

does not split into two parts. $\langle S_{ib}^z(t) \rangle_f$ (spin-flip case) and $\langle S_{ib}^z(t) \rangle$ (without spin-flip) move with similar speeds (see Fig. 5(d)).

Conclusions. Using the Krylov-space t-DMRG method we studied the real-time dynamics of an excitonic wave-packet evolving via a two-orbital Hubbard model on a chain, at intermediate coupling U/W . We observed the real-space spin-orbit and spin-charge separation by monitoring the dynamics of spin, charge, and orbital wave-packets. We find that the charge and spin wave-packets of the higher energy orbital a move together, whereas the charge and spin wave-packets of the lower energy orbital b moves in opposite direction (Fig. 6). The electron in the higher energy orbital and hole in the lower energy orbital always moves together. The inter-orbital interactions (U' and J_H) play a crucial role in orbiton dynamics. For example, the orbiton velocity increases significantly by increasing J_H/U , whereas the spinon velocity remains unchanged. Interestingly, we found that *a hole in a one-orbital chain moves much faster than a hole in a two-orbital chain*, because the hole in the lower energy orbital forms a (heavy) bound pair with the electron in the higher energy orbital. Moreover, we presented the dynamics of the spin-flipped exciton, where we found evidence of fractional spinons at large Hund's coupling. Our calculations will be extended in future work in various directions. For example, into other chain multiorbital systems with exotic states [33], including spin-orbit coupling [34], into ladder geometries [35], in materials with orbital order [36], ruthenates [37], and into generic $t - J$ models [38].

Acknowledgments. We thank N. Kaushal and N. D. Patel for discussions. B.P. and E.D. were supported by the U.S. Department of Energy (DOE), Office of Science, Basic Energy Sciences (BES), Materials Sciences and Engineering Division. G.A. was partially supported by the Center for Nanophase Materials Sciences, which is a U.S. DOE Office of Science User Facility, and by the Scientific Discovery through Advanced Computing (SciDAC) program funded by U.S. DOE, Office of Science, Advanced Scientific Computing Research and Basic Energy Sciences, Division of Materials Sciences and Engineering. Validation and some computer runs were conducted at the Center for Nanophase Materials Sciences, which is a DOE Office of Science User Facility.

-
- [1] C. Kim, A. Y. Matsuura, Z.-X. Shen, N. Motoyama, H. Eisaki, S. Uchida, T. Tohyama, and S. Maekawa, Phys. Rev. Lett. **77**, 4054 (1996). <https://doi.org/10.1103/PhysRevLett.77.4054>
 - [2] Y. Tokura and N. Nagaosa, Science **288**, 462 (2000). <https://doi.org/10.1126/science.288.5465.462>
 - [3] B. J. Kim, H. Koh, E. Rotenberg, S.-J. Oh, H. Eisaki, N. Motoyama, S. Uchida, T. Tohyama, S. Maekawa, Z.-

- X. Shen and C. Kim, Nat. Phys. **2**, 397 (2006). <https://doi.org/10.1038/nphys316>
- [4] Y. Matiks, P. Horsch, R. K. Kremer, B. Keimer, and A. V. Boris, Phys. Rev. Lett. **103**, 187401 (2009). <https://doi.org/10.1103/PhysRevLett.103.187401>
- [5] F. C. Zhang and K. K. Ng, Phys. Rev. B **58**, 13520 (1998). <https://doi.org/10.1103/PhysRevB.58.13520>
- [6] J. Rincón, E. Dagotto, and A. E. Feiguin, Phys. Rev. B **97**, 235104 (2018). <https://doi.org/10.1103/PhysRevB.97.235104>
- [7] E. Collart, A. Shukla, J.-P. Rueff, P. Leininger, H. Ishii, I. Jarrige, Y. Q. Cai, S.-W. Cheong, and G. Dhalenne, Phys. Rev. Lett. **96**, 157004 (2006). <https://doi.org/10.1103/PhysRevLett.96.157004>
- [8] Jungho Kim, D. Casa, M. H. Upton, T. Gog, Young-June Kim, J. F. Mitchell, M. van Veenendaal, M. Daghofer, J. van den Brink, G. Khaliullin, and B. J. Kim, Phys. Rev. Lett. **108**, 177003 (2012). <https://doi.org/10.1103/PhysRevLett.108.177003>
- [9] Jungho Kim, M. Daghofer, A.H. Said, T.Gog, J. van den Brink, G. Khaliullin and B.J. Kim, Nat. Commun. **5**, 4453 (2014). <https://doi.org/10.1038/ncomms5453>
- [10] T. Giamarchi, Quantum Physics in One Dimension (Clarendon, Oxford, 2004). <https://doi.org/10.1093/acprof:oso/9780198525004.001.0001>
- [11] F.D.M. Haldane, J. Phys. C **14**, 2585 (1981). <https://doi.org/10.1088/0022-3719/14/19/010>
- [12] B. Pandey, E. Dagotto, and S. K. Pati, Phys. Rev. B **102**, 214302 (2020). <https://doi.org/10.1103/PhysRevB.102.214302>
- [13] J. Voit, Phys. Rev. B **47**, 6740 (1993). <https://doi.org/10.1103/PhysRevB.47.6740>
- [14] E. A. Jagla, K. Hallberg, and C. A. Balseiro, Phys. Rev. B **47**, 5849 (1993). <https://doi.org/10.1103/PhysRevB.47.5849>
- [15] K. A. Al-Hassanieh, J. Rincón, E. Dagotto, and G. Alvarez, Phys. Rev. B **88**, 045107 (2013). <https://doi.org/10.1103/PhysRevB.88.045107>
- [16] O. M. Auslaender, H. Steinberg, A. Yacoby, Y. Tserkovnyak, B. I. Halperin, K. W. Baldwin, L. N. Pfeiffer, and K. W. West, Science **308**, 88 (2005). <https://doi.org/10.1126/science.1107821>
- [17] C. Kollath, U. Schollwöck, and W. Zwerger, Phys. Rev. Lett. **95**, 176401 (2005). <https://doi.org/10.1103/PhysRevLett.95.176401>
- [18] J. Schlappa, K. Wohlfeld, K. J. Zhou, M. Mourigal, M. W. Haverkort, V. N. Strocov, L. Hozoi, C. Monney, S. Nishimoto, S. Singh, A. Revcolevschi, J.-S. Caux, L. Patthey, H. M. Rønnow, J. van den Brink and T. Schmitt, Nature **485**, 82 (2012). <https://doi.org/10.1038/nature10974>
- [19] V. Bisogni, K. Wohlfeld, S. Nishimoto, C. Monney, J. Trinckauf, K. Zhou, R. Kraus, K. Koepf, C. Sekar, V. Strocov, B. Büchner, T. Schmitt, J. van den Brink, and J. Geck, Phys. Rev. Lett. **114**, 096402 (2015). <https://doi.org/10.1103/PhysRevLett.114.096402>
- [20] K. Wohlfeld, M. Daghofer, S. Nishimoto, G. Khaliullin, and J. van den Brink, Phys. Rev. Lett. **107**, 147201 (2011). <https://doi.org/10.1103/PhysRevLett.107.147201>
- [21] J. Heverhagen and M. Daghofer, Phys. Rev. B **98**, 085120 (2018). <https://doi.org/10.1103/PhysRevB.98.085120>
- [22] R. Fumagalli, J. Heverhagen, D. Betto, R. Arpaia, M. Rossi, D. Di Castro, N. B. Brookes, M. Moretti Sala, M. Daghofer, L. Braicovich, K. Wohlfeld, and G. Ghiringhelli, Phys. Rev. B **101**, 205117 (2020). <https://doi.org/10.1103/PhysRevB.101.205117>
- [23] S. R. White and Adrian E. Feiguin, Phys. Rev. Lett. **93**, 076401 (2004). <https://doi.org/10.1103/PhysRevLett.93.076401>
- [24] A. E. Feiguin and S. R. White, Phys. Rev. B **72**, 020404(R) (2005). <https://doi.org/10.1103/PhysRevB.72.020404>
- [25] Q. Luo, A. Nicholson, J. Rincón, S. Liang, J. Riera, G. Alvarez, L. Wang, W. Ku, G. D. Samolyuk, A. Moreo, and E. Dagotto Phys. Rev. B **87**, 024404 (2013). <https://doi.org/10.1103/PhysRevB.87.024404>
- [26] G. Alvarez, Luis G. G. V. Dias da Silva, E. Ponce, and E. Dagotto, Phys. Rev. E **84**, 056706 (2011). <https://doi.org/10.1103/PhysRevE.84.056706>
- [27] G. Alvarez, Comput. Phys. Commun. **180**, 1572 (2009). <https://doi.org/10.1016/j.cpc.2009.02.016>
- [28] This robust Hund coupling is commonly used in the context of iron-based superconductors, see Q. Luo, G. Martins, D.-X. Yao, M. Daghofer, R. Yu, A. Moreo, and E. Dagotto, Phys. Rev. B **82**, 104508 (2010) and references therein. <https://doi.org/10.1103/PhysRevB.82.104508>
- [29] C. Yang and A. E. Feiguin, Phys. Rev. B **98**, 035128 (2018). <https://doi.org/10.1103/PhysRevB.98.035128>
- [30] C. Lane and Jian-Xin Zhu, Phys. Rev. B **101**, 155135 (2020). <https://doi.org/10.1103/PhysRevB.101.155135>
- [31] These differences highlight the importance of studying a Hubbard model because the intermediate and strong coupling regimes do not necessarily behave equally.
- [32] C.-C. Chen, M. van Veenendaal, T. P. Devereaux, and K. Wohlfeld, Phys. Rev. B **91**, 165102 (2015). <https://doi.org/10.1103/PhysRevB.91.165102>
- [33] See for example B. Pandey, L-F. Lin, R. Soni, N. Kaushal, J. Herbrych, G. Alvarez, and E. Dagotto, Phys. Rev. B **102**, 035149 (2020) <https://doi.org/10.1103/PhysRevB.102.035149>; N. D. Patel, N. Kaushal, A. Nocera, G. Alvarez, and E. Dagotto, npj Quantum Mater. **5**, 27 (2020) <https://doi.org/10.1038/s41535-020-0228-2>; J. Herbrych, J. Heverhagen, G. Alvarez, M. Daghofer, A. Moreo, and E. Dagotto, Proc. Natl. Acad. Sci. USA **117**, 16226 (2020) <https://doi.org/10.1073/pnas.2001141117>; J. Herbrych, J. Heverhagen, N. D. Patel, G. Alvarez, M. Daghofer, A. Moreo, and E. Dagotto, Phys. Rev. Lett. **123**, 027203 (2019) <https://doi.org/10.1103/PhysRevLett.123.027203>; J. Herbrych, G. Alvarez, A. Moreo, and E. Dagotto, Phys. Rev. B **102**, 115134 (2020) <https://doi.org/10.1103/PhysRevB.102.115134>; M. Sroda, E. Dagotto, and J. Herbrych, Phys. Rev. B **104**, 045128 (2021) <https://doi.org/10.1103/PhysRevB.104.045128>.
- [34] N. Kaushal, A. Nocera, G. Alvarez, A. Moreo, and E. Dagotto, Phys. Rev. B **99**, 155115 (2019). <https://doi.org/10.1103/PhysRevB.99.155115>
- [35] See for example N.D. Patel, A. Nocera, G. Alvarez, A. Moreo, S. Johnston, and E. Dagotto, Comm. Phys. (Nature) **2**, 64 (2019) <https://doi.org/10.1038/s42005-019-0155-3>; B. Pandey, R. Soni, L-F. Lin, G. Alvarez, and E. Dagotto, Phys.

- Rev. B **103**, 214513 (2021)<https://doi.org/10.1103/PhysRevB.103.214513>; Y. Zhang, L.-F. Lin, A. Moreo, S. Dong, and E. Dagotto, Phys. Rev. B **100**, 184419 (2019) <https://doi.org/10.1103/PhysRevB.100.184419>; Y. Zhang, L-F. Lin, A. Moreo, S. Dong, and E. Dagotto, Phys. Rev. B **101**, 144417 (2020)<https://doi.org/10.1103/PhysRevB.101.144417> .
- [36] L.-F. Lin, N. Kaushal, Y. Zhang, A. Moreo, and E. Dagotto, Phys. Rev. Materials **5**, 025001 (2021). <https://doi.org/10.1103/PhysRevMaterials.5.025001>
- [37] T. Hotta and E. Dagotto, Phys. Rev. Lett. **88**, 017201 (2001). <https://doi.org/10.1103/PhysRevLett.88.017201>
- [38] J. Riera, K. Hallberg, and E. Dagotto, Phys. Rev. Lett. **79**, 713 (1997). <https://doi.org/10.1103/PhysRevLett.79.713>